

# Plasma induced damage mitigation in spin-on self-assembly based ultra low-k dielectrics using template residues

M. Krishtab,<sup>1,2,a)</sup> J.-F. de Marneffe,<sup>1</sup> S. De Gendt,<sup>1,2</sup> and M. R. Baklanov<sup>b)</sup>

<sup>1</sup> Imec, Kapeldreef 75, Leuven 3001, Belgium

<sup>2</sup> KU Leuven, Department of Chemistry, Celestijnenlaan 200F, Leuven 3001, Belgium

This paper describes an approach for the reduction of plasma-induced damage in self-assembly based porous ultra low-k organosilica dielectrics. The concept is based on retention of the partially decomposed sacrificial organic phase (template) into the pores of the low-k film during plasma exposure. The amount of the template residues can be controlled by varying the hard-bake process time. It is shown that those residues are uniformly distributed throughout the film in the form of pore wall coatings. After plasma processing, the remaining residues are removed by means of a UV cure. Plasma damage to the underlying organosilica matrix was assessed by exposure of the differently hard-baked low-k films to fluorine-rich Ar/SF<sub>6</sub> plasma. The thickest coating, estimated to be around 0.4 nm, enables a nearly damage-free etch process without any carbon depletion or k-value degradation along with limited shrinkage induced by post-etch UV-curing (< 4.5%). These results highlight the efficiency of a simple and scalable route for damage-free integration of highly porous self-assembly based low-k dielectrics.

The degradation of intrinsic properties of porous organosilica (OSG) low-k dielectrics during patterning process is one of the key challenges for integration of these materials into the damascene interconnects fabrication process.<sup>1</sup> The problem is particularly severe for ultra low-k dielectrics with porosity exceeding 20-30%, i. e. beyond the percolation threshold.<sup>2</sup> In this case the pores become fully interconnected which allows deep penetration of damaging plasma species and extraction of organic groups from the OSG matrix.<sup>3</sup> Over the last decade, different strategies for the mitigation of plasma damage to the low-k dielectrics have been investigated. The proposed

<sup>a)</sup> Author to whom correspondence should be addressed. Electronic mail: mikhail.krishtab@imec.be

<sup>b)</sup> The research was performed while M. R. Baklanov was at imec, Kapeldreef 75, Leuven 3001, Belgium

solutions can be roughly grouped in two categories. The first one includes the methods focused on optimization of a particular element of the low-k patterning process, e. g. the plasma chemistry, the composition/structure of the dielectric or the introduction of a post-etch low-k restoration process. Another group of methods rely on a conceptually different approach for the processing or patterning of the porous dielectric. The unifying idea of these methods is a temporary, partial or complete elimination of porosity. The first example, adopted from the membrane community, is the temporary addition of extra polymer, i.e. the Post-Porosity Plasma Protection (P4)<sup>4,5</sup> technique, where pore “stuffing” and “de-stuffing” steps are added to the interconnect flow; in another example porous dielectric densification occurs through in-situ capillary condensation of reagents gases and/or etch by-products at cryogenic temperatures.<sup>6,7</sup> Other approaches inspired by the same principle are post-integration porogen removal<sup>8,9</sup> and effective porogen control (EPC)<sup>10</sup> strategies which rely on etching of the low-k film with a fully or partially preserved sacrificial phase. Unlike the P4 and cryogenic etching schemes, the latter approaches are less universal and their performance in terms of k-value preservation and post-etch film shrinkage is strongly linked to the type of low-k employed. So far the efficiency of these approaches was briefly demonstrated on PECVD films as well as spin-on dielectrics with acrylic polymers based nanoparticles. In this work we investigate a similar approach applied to a solution-processed low-k material, formation of which involves co-self-assembly of templating surfactant molecules and organosilica precursors.<sup>11,12</sup> An outstanding representative of such dielectric materials is a family of periodic mesoporous organosilicas (PMOs), which are being actively investigated as a potential successor of PECVD dielectrics into advanced technology nodes.<sup>13-15</sup> We showed that the partially decomposed polyethylene oxide based surfactant molecules commonly used during PMO synthesis<sup>16</sup> can act as an efficient plasma protective phase and can be completely removed after the etching step, thus creating prerequisites for damage-free patterning of the self-assembly based low-k films.

The SOG-2.2 low-k films targeting the k-value of 2.2 were deposited on 300mm n-type Si wafers from a sol containing a mixture of organosilica esters and amphiphilic molecules as template. The molecules consist of linear hydrophilic and hydrophobic blocks represented by polyethylene oxide and a saturated hydrocarbon chain, respectively. After spin-coating and short low temperature annealing in air (soft-bake), the films were sintered at 400°C in N<sub>2</sub> (further referred as hard-baked or HB) for different times to capture various stages of the template decomposition. The combination of 120 min hard-bake with an additional UV-curing ( $\lambda > 200$  nm) at a susceptor temperature of 385°C for 2 minutes (further referred as UV) was used as a reference condition producing a

mechanically stable and template free low-k film. Due to the additional heating induced by UV-absorption, the actual wafer temperature during the UV-curing process was about 400°C. The low-k films were characterized using FTIR spectroscopy (Nicolet 6800), spectroscopic ellipsometry (Sentech SE801) and ellipsometric porosimetry with toluene as adsorbate<sup>17</sup>. To evaluate the protective role of the template residues, the obtained films were exposed to an Ar/SF<sub>6</sub> discharge in a commercial magnetically enhanced dual-frequency CCP reactor Vesta™ from Tokyo Electron Ltd. The plasma was ignited and maintained at 120 mTorr using total power of 500W (400W + 100W of 100 MHz and 13.67 MHz RF power supplies, respectively) and equal flows of Ar and SF<sub>6</sub> gases set to 100 sccm. Apart from ellipsometry and FTIR, the analysis of the plasma induced damage was performed with TOF SIMS depth profiling (TOFSIMS IV from ION-TOF GmbH operating in dual beam configuration) and complemented with HF-dipping test (aqueous 0.2% HF, 60s) revealing the thickness of the carbon-depleted low-k layer.<sup>18</sup> Dielectric constant of the low-k films was estimated from capacitance measured with E4980A Precision LCR Meter on planar metal-insulator-semiconductor structures formed by evaporation of 70 nm Pt contact pads on top of n-Si/SOG-2.2 stacks.<sup>19</sup>

The proposed approach relies on three key elements: fast OSG matrix cross-linking compared to the template decomposition rate; the protective role of the incompletely decomposed sacrificial phase; and the complete template residues removal during the post-etch UV-curing step.

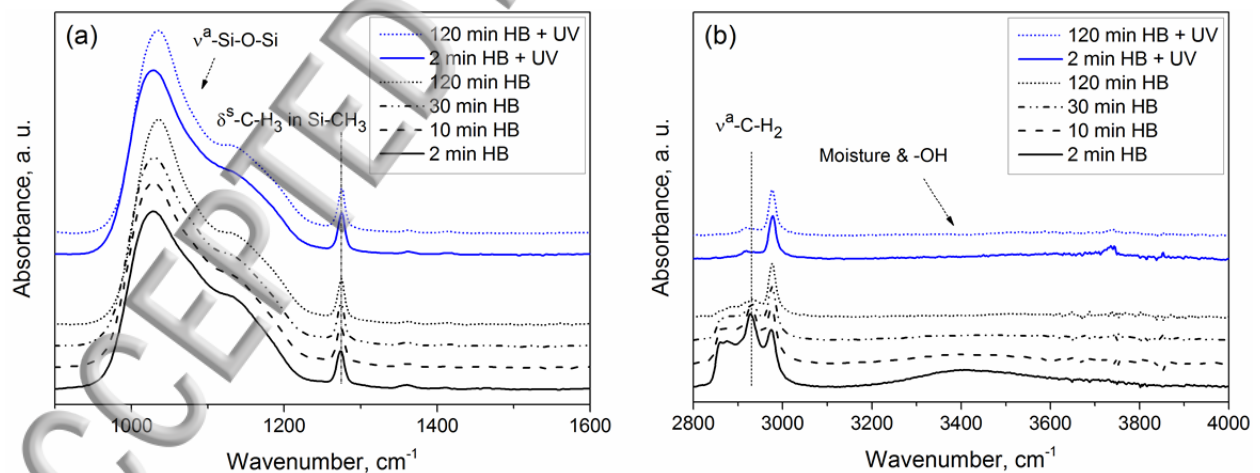


FIG. 1. IR-absorbance spectra of SOG-2.2 low-k films hard-baked (HB)/ hard-baked and UV-cured (HB+UV) for different times.

To address the first element, we investigated how the properties of the SOG-2.2 films evolve as a function of hard-bake time. Compositional changes of both the organosilica matrix and the sacrificial phase can be measured by

FTIR, see Figure 1. The absorbance in the wavenumber range  $1000-1150\text{ cm}^{-1}$  corresponding to asymmetric Si-O-Si bond stretching<sup>20</sup> experiences no significant changes already after the shortest tested hard-bake time (Figure 1a). Meanwhile the absorbance from asymmetric C-H stretching in  $-\text{CH}_2-$  group at around  $2925\text{ cm}^{-1}$ ,<sup>20</sup> which can be largely associated with the sacrificial phase in the pores, reduces continuously over 2 hours of hard-bake (Figure 1b). Another critical aspect such as template removal efficiency of the UV-curing was assessed by applying this treatment to the hard-baked SOG-2.2 films containing the smallest and the largest amount of sacrificial phase, i. e. hard-baked for 2 and 120 minutes. After UV cure, both films show the lowest FTIR absorbance in the range of wavenumbers corresponding to  $-\text{CH}_2-$  groups indicating effective removal of the template.

TABLE I. Properties of SOG-2.2 films prepared under different conditions of the hard-bake sequence.

Hard-bake sequence	Thickness, nm	Pore radius, nm	Open porosity, %
0 min HB	$217.8 \pm 0.9$	-	-
2 min HB	$195.3 \pm 2.1$	0.8	25.6
10 min HB	$193.3 \pm 2.0$	0.9	27.7
30 min HB	$192.6 \pm 1.9$	0.9	31.1
120 min HB	$192.0 \pm 0.9$	1.1	35.0
2 min HB + UV	$191.1 \pm 2.0$	1.1	38.6
120 min HB + UV	$191.8 \pm 0.5$	1.2	37.9

More evidence supporting the results of FTIR analysis can be found in Table I. After 2 minutes bake, the film thickness reduces from  $\sim 218\text{ nm}$  down to  $\sim 195\text{ nm}$ , 2-3 nm above the steady-state value of  $\sim 192\text{ nm}$  reached after long bake, indicating that most film shrinkage occurs over the first two minutes of the hard-bake, due to the condensation of unreacted silanol (Si-OH) groups. For extended bake time, the thickness variation does not exceed 3%, which indicates that the OSG matrix is largely cross-linked and mechanically robust after only 2 min hard-bake. Such fast matrix hardening can be attributed to well-defined separation between the sacrificial template phase and the OSG matrix. This is generally prone to the self-assembly based spin-on low-k films and is even more prominent in the SOG-2.2 material under test because of relatively short PEO-block within the surfactant molecule.<sup>21</sup> Considered together with FTIR results, these data indicate clearly that the OSG matrix cross-linking is a fast phenomenon while sacrificial organics have decomposition rate at least one order of magnitude slower.

Regarding the pore structure of the hard-baked films, it can be noted that both open porosity and average pore radius simultaneously increase with hard-bake time. This supports the assumption of the uniform distribution of the template residues throughout the SOG-2.2 layer (validated in the next section). In turn, it makes it feasible to assume that the template residues stay in the low-k films as pore wall coating. The thickness of this coating can be roughly estimated as a difference between the average pore radii measured in the film of interest and in the film cleaned from the template residues by long hard-bake and additional UV-curing. Following this approach, we calculated that after 2 min hard-bake the template residues take up to 30% of the open porous volume and cover the pore walls with a layer of about 0.3-0.4 nm thick. Another important remark about the pore structure which should be made before discussing the interaction of the low-k films with plasma is related to the organization of the porous volume. It was found that SOG-2.2 films have disordered “worm-like” pore arrangement (Figure S1 in Supplementary Material) which implies vertical interconnectivity of the pore channels and thus makes it susceptible to the diffusion of plasma-generated species.

The second key element addresses the ability of the template residue coatings to protect the OSG matrix from plasma processing, with emphasis on highly damaging  $F^*$  radicals. Samples with different levels of template residues (Table I) were exposed to the  $Ar/SF_6$  plasma for 35s (further referred as ETCH), then half of the etched samples was UV-cured to get template-free low-k films. To evidence the carbon-depleted top layer formed during the etch process, the UV-cured samples were pre-measured with ellipsometry and then immersed into 0.2% aqueous HF solution for 60s. The observed thickness loss gives an estimate of the low-k damage depth. As can be seen in Figure 2, the thickness loss caused by HF-dip inversely correlates with the amount of the template residues present in the low-k films during etching. The largest damage depth of approximately 52 nm is found in the SOG-2.2 layer UV-cured prior to the etch process, while this value is about 10 times smaller for the film hard-baked for 2 minutes and hosting ~30% of the templating organics.

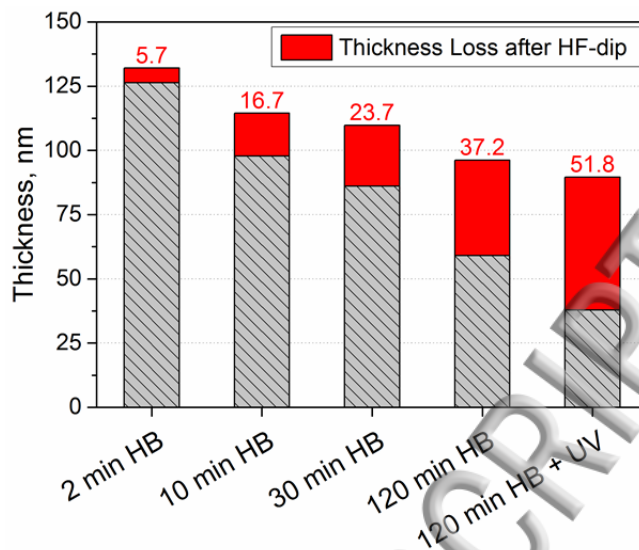


FIG. 2. The thickness of the SOG-2.2 films after 35s Ar/SF<sub>6</sub> etch and post-etch UV-treatment (pristine thickness ~ 200nm). The part of the film removed by subsequent 0.2% HF dip is indicated in red.

While the HF-dip test provides an indirect indication of the carbon depletion, TOF-SIMS depth profiling gives a better insight into the carbon distribution within the low-k layer. Figure 3 shows the C<sup>-</sup> intensity as a function of sputter time for the films with the largest and the smallest tested amount of the template residues retained before the etch process, i. e. for the hard-bake sequences referred in Table I as “2 min HB” and “120 min HB + UV”, respectively. The level of carbon is compared at two process stages – after hard-bake and after etching followed by UV-cure step. In case the films followed just the hard-bake sequence, the carbon intensity remains more or less constant throughout the layer, thus confirming the uniform decomposition of the sacrificial organic template during the hard-bake annealing. As expected, the most significant changes in the carbon profiles appear after plasma etch. In agreement with the results of HF-dip test, the carbon depletion is particularly significant in the material containing the lowest amount of the template residues before etching. In this case the depleted region exceeds half of the film thickness. On the contrary, the C loss is almost negligible in the case of the film hard-baked for 2 minutes.

To make sure that the carbon preserved in the organosilica matrix during etching is still present in its original form (Si-CH<sub>3</sub> groups), FTIR spectra of the samples before and after the plasma exposure were compared, as shown in Figure 4. Although the initial height and position of Si-CH<sub>3</sub> peak at around 1275 cm<sup>-1</sup> slightly varies (which might be related to proximity of the template residues), the relative absorbance changes caused by the plasma can be compared. The spectra support the previous findings and additionally provide an evidence of the largely intact

matrix organics in the case of 2 min hard-baked film. The slight decrease of the peak intensity after etching can be attributed to partial replacement of Si-CH<sub>3</sub> groups with Si-H, Si-OH or its fluorinated form Si-CH<sub>x</sub>F<sub>3-x</sub>. However since neither Si-H, Si-OH or concomitant moisture appear in the full spectra (not shown), the fluorination is the most plausible chemical change.

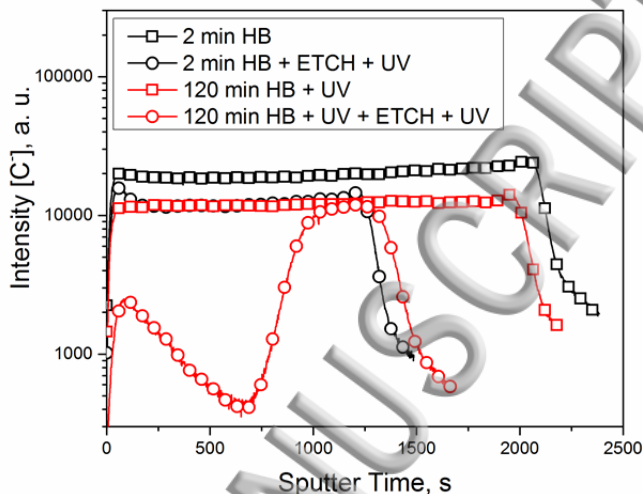


FIG. 3. TOF SIMS carbon (C) depth profiles recorded as a function of sputter time on SOG-2.2 low-k films which followed different hard-bake sequence and identical etch process with successive UV-cure.

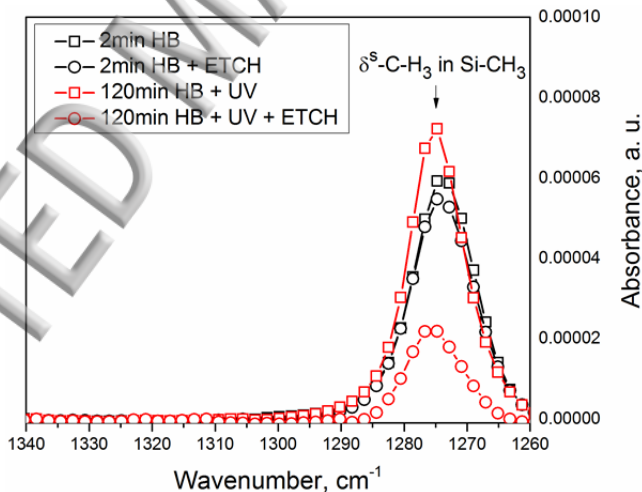


FIG. 4. The IR absorbance peak (normalized by the film thickness) corresponding to C-H vibrations within Si-CH<sub>3</sub> group recorded on SOG-2.2 films before and after exposure to Ar/SF<sub>6</sub> plasma.

In order to understand the underlying damage reduction mechanism we need to refer to the plasma conditions used. The plasma-induced damage of the porous organosilica material is attributed to different interactions with species generated in the discharge, i.e. free reactive radicals, ions or VUV photons. In the case of Ar/SF<sub>6</sub> plasma

used in this work, the impact of fluorine radicals is considered as the dominating low-k damage mechanism due to strong plasma dissociation of the SF<sub>6</sub> molecule<sup>22</sup> compared to the relatively low VUV-induced damage caused by small fraction of Ar in the total flow.<sup>23</sup> The interaction between F-radicals and porous silica-based low-k films has been recently well described by Rakhimova *et al.*<sup>24,25</sup> Exposure to F-radicals forms the carbon depleted layer in low-k film as a result of two propagating processes – fluorination of Si-CH<sub>3</sub> groups as well as the material etching via elimination of –CF<sub>3</sub> groups and subsequent reaction with the exposed Si-O bonds of the matrix. The rate of both processes, relying on diffusion of F-radicals, is strongly affected by the pore structure of the low-k dielectric. As a consequence, the protective impact of the template residue coating can be attributed to the substantially reduced open porosity and pore dimensions, reducing significantly F\* diffusion through the porous matrix. In addition, the presence of sacrificial organics covering the pore walls could also sterically hinder the fluorination of Si-CH<sub>3</sub> groups thus protecting the organosilica matrix from unwanted modification even at the topmost part of the low-k film where the concentration of fluorine radicals is the highest.

TABLE II. k-values and film shrinkage induced by post-etch UV-curing.

Processing sequence	k-value (100 kHz)	Shrinkage , %
120 min HB + UV	2.21 ± 0.07	-
2 min HB + ETCH + UV	2.22 ± 0.07	4.5
30 min HB + ETCH + UV	2.64 ± 0.08	1.6
120 min HB + UV + ETCH + UV	3.09 ± 0.09	0.8

Finally, to assess the applicability of the proposed low-k patterning sequence, we measured the dielectric constant after the complete low-k processing and estimated the film shrinkage caused by the post-etch template removal by UV-cure (Table II). The latter should be minimized to exclude the potential risk of hard-mask delamination or undesirable variation of the etch profile. The preserved k-value in the case of 2 min hard-baked SOG-2.2 comes at the expense of the film shrinkage of about 4% which is twice lower than the value reported for the late porogen removal approach.<sup>9</sup>

In summary, this work demonstrates that the partial decomposition of the typical PEO-based templating molecules during hard-bake of self-assembly based low-k dielectrics leads to formation of protective organic coatings. These are uniformly covering the pore surface of a mechanically robust OSG matrix. The resulting modified pore structure as well as passivation of the matrix minimizes its interaction with diffusing reactive F\*

plasma radicals. By optimization of hard-bake time, we achieved nearly damage-free plasma etching of highly porous dielectric films. The additional post-etch UV-curing step efficiently removes the remaining template residues. We believe, that the proposed strategy based on simple modification of the standard damascene metallization flow could be of special interest for integration of such promising sub-class of self-assembly based low-k dielectrics as PMOs.

### SUPPLEMENTARY MATERIAL

See Supplementary Material for the details of SOG-2.2 film pore structure and for the dielectric constants of the low-k films before plasma etching.

### ACKNOWLEDGMENTS

The authors would like to thank SBA Materials Inc. for providing the sols used for deposition of the low-k dielectric films and Alexis Franquet from MCA department of imec for performing TOF SIMS measurements.

### REFERENCES

- <sup>1</sup> M.R. Baklanov, J.-F. de Marneffe, D. Shamiryman, A.M. Urbanowicz, H. Shi, T. V. Rakhimova, H. Huang, and P.S. Ho, *J. Appl. Phys.* **113**, 41101 (2013).
- <sup>2</sup> K.H. Lee, J.H. Yim, and M.R. Baklanov, *Microporous Mesoporous Mater.* **94**, 113 (2006).
- <sup>3</sup> M. Darnon, N. Casiez, T. Chevolleau, G. Dubois, W. Volksen, T.J. Frot, R. Hurand, T.L. David, N. Posseme, N. Rochat, and C. Licitra, *J. Vac. Sci. Technol. B Microelectron. Nanom. Struct.* **31**, 11207 (2013).
- <sup>4</sup> T. Frot, W. Volksen, T. Magbitang, D. Miller, S. Purushothaman, M. Lofaro, R. Bruce, and G. Dubois, in *2011 IEEE Int. Interconnect Technol. Conf.* (IEEE, 2011), pp. 1–3.
- <sup>5</sup> L. Zhang, J.-F. de Marneffe, M.H. Heyne, S. Naumov, Y. Sun, A. Zotovich, Z. el Otell, F. Vajda, S. De Gendt, and M.R. Baklanov, *ECS J. Solid State Sci. Technol.* **4**, N3098 (2014).
- <sup>6</sup> L. Zhang, R. Ljazouli, P. Lefauchaux, T. Tillocher, R. Dussart, Y. a. Mankelevich, J.-F. de Marneffe, S. de Gendt,

and M.R. Baklanov, ECS Solid State Lett. **2**, N5 (2012).

<sup>7</sup> L. Zhang, J.-F. de Marneffe, F. Leroy, P. Lefauchaux, T. Tillocher, R. Dussart, K. Maekawa, K. Yatsuda, C. Dussarrat, A. Goodyear, M. Cooke, S. De Gendt, and M.R. Baklanov, J. Phys. D: Appl. Phys. **49**, 175203 (2016).

<sup>8</sup> V. Jousseume, M. Assous, A. Zenasni, S. Maitrejean, B. Remiat, P. Leduc, H. Trouve, C. Le Cornec, M. Fayolle, A. Roule, F. Ciaramella, D. Bouchu, T. David, A. Roman, D. Scevola, T. Morel, D. Rebiscoul, G. Prokopowicz, M. Jackman, C. Guedj, D. Louis, M. Gallagher, and G. Passemard, in *Proc. IEEE 2005 Int. Interconnect Technol. Conf. 2005*. (IEEE, 2005), pp. 60–62.

<sup>9</sup> V. Jousseume, L. Favennec, A. Zenasni, and G. Passemard, Appl. Phys. Lett. **88**, (2006).

<sup>10</sup> Y. Kagawa, Y. Enomoto, T. Shimayama, T. Kameshima, M. Okamoto, H. Kawshima, A. Yamada, T. Hasegawa, K. Akiyama, H. Masuda, M. Miyajima, H. Shibata, and S. Kadomura, in *2006 Int. Interconnect Technol. Conf.* (IEEE, 2006), pp. 207–209.

<sup>11</sup> Y. Lu, R. Ganguli, C. Drewien, M.T. Anderson, C. Brinker, W. Gong, Y. Guo, H. Soyez, B. Dunn, M. Huang, and J. Zink, Nature **389**, 364 (1997).

<sup>12</sup> D. Grosso, F. Cagnol, G.J. de A.A. Soler-Illia, E.L. Crepaldi, H. Amenitsch, a. Brunet-Bruneau, a. Bourgeois, and C. Sanchez, Adv. Funct. Mater. **14**, 309 (2004).

<sup>13</sup> B.D. Hatton, K. Landskron, W. Whitnall, D.D. Perovic, and G.A. Ozin, Adv. Funct. Mater. **15**, 823 (2005).

<sup>14</sup> W. Wang, D. Grozea, S. Kohli, D.D. Perovic, and G. a Ozin, ACS Nano **5**, 1267 (2011).

<sup>15</sup> J.M. Torres, J. Bielefeld, J. Blackwell, D.J. Michalak, and J.S. Clarke, in *2016 IEEE Int. Interconnect Technol. Conf. / Adv. Met. Conf.* (IEEE, 2016), pp. 18–20.

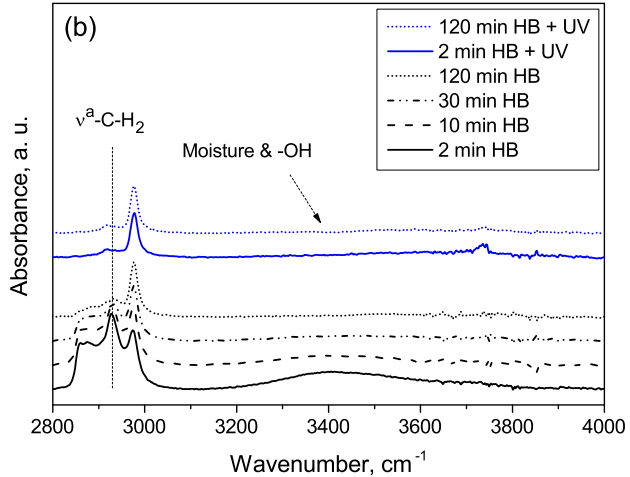
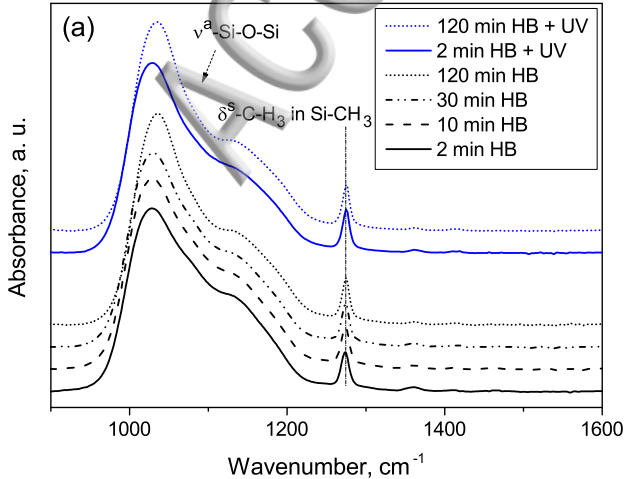
<sup>16</sup> P. Van der Voort, D. Esquivel, E. De Canck, F. Goethals, I. Van Driessche, and F.J. Romero-Salguero, Chem. Soc. Rev. **42**, 3913 (2013).

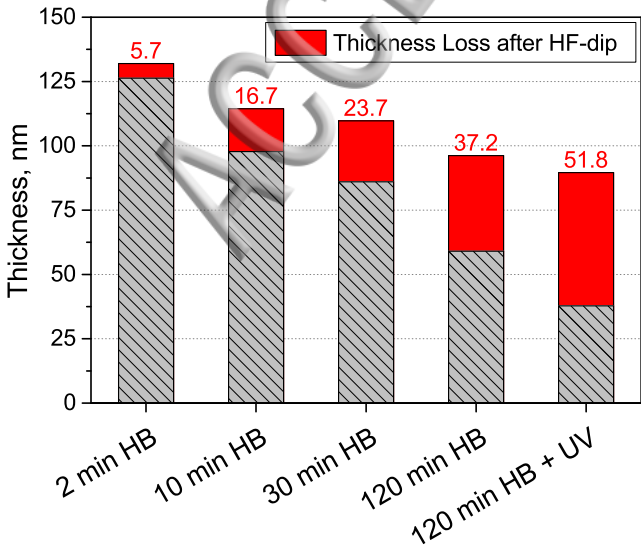
<sup>17</sup> M.R. Baklanov, K.P. Mogilnikov, V.G. Polovinkin, and F.N. Dultsev, J. Vac. Sci. Technol. B **18**, 1385 (2000).

<sup>18</sup> Q.T. Le, M.R. Baklanov, E. Kesters, a. Azioune, H. Struyf, W. Boullart, J.-J. Pireaux, and S. Vanhaelemeersch, Electrochem. Solid-State Lett. **8**, F21 (2005).

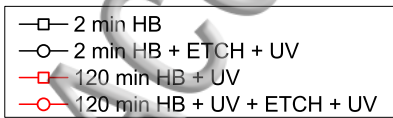
<sup>19</sup> I. Ciofi, M.R. Baklanov, Z. Tőkei, and G.P. Beyer, Microelectron. Eng. **87**, 2391 (2010).

- <sup>20</sup> Grill and D. a. Neumayer, J. Appl. Phys. **94**, 6697 (2003).
- <sup>21</sup> V.R. Koganti, S. Das, and S.E. Rankin, J. Phys. Chem. C **118**, 19450 (2014).
- <sup>22</sup> L.G. Christophorou, J. Phys. Chem. Ref. Data **29**, 553 (2000).
- <sup>23</sup> J.-F. de Marneffe, L. Zhang, M. Heyne, M. Lukaszewicz, S.B. Porter, F. Vajda, V. Rutigliani, Z. el Otell, M. Krishtab, A. Goodyear, M. Cooke, P. Verdonck, and M.R. Baklanov, J. Appl. Phys. **118**, 133302 (2015).
- <sup>24</sup> T. V Rakhimova, D. V Lopaev, Y.A. Mankelevich, A.T. Rakhimov, S.M. Zyryanov, K.A. Kurchikov, N.N. Novikova, and M.R. Baklanov, J. Phys. D. Appl. Phys. **48**, 175203 (2015).
- <sup>25</sup> T. V Rakhimova, D. V Lopaev, Y. a Mankelevich, K. a Kurchikov, S.M. Zyryanov, a P. Palov, O. V Proshina, K.I. Maslakov, and M.R. Baklanov, J. Phys. D. Appl. Phys. **48**, 175204 (2015).





Intensity [C], a. u.



Sputter Time, s

100000

10000

1000

0

500

1000

1500

2000

2500

